Arabian Journal of Chemistry (2019) **12**, 1011–1023

King Saud University

Arabian Journal of Chemistry

www.ksu.edu.sa
www.sciencedirect.com

ORIGINAL ARTICLE

Fabrication and characterization of supported dual acidic ionic liquids for polymer electrolyte membrane fuel cell applications

Masoumeh Zakeri [a], Ebrahim Abouzari-Lotf [b,c,*], Mohamed Mahmoud Nasef [b,d,*], Arshad Ahmad [b,c], Mikio Miyake [a], Teo Ming Ting [e], Paveswari Sithambaranathan [b,c]

[a] *Malaysia–Japan International Institute of Technology, Universiti Teknolog Malaysia, 54100 Kuala Lumpur, Malaysia*
[b] *Advanced Materials Research Group, Center of Hydrogen Energy, Institute of Future Energy, Universiti Teknologi Malaysia, 54100 Kuala Lumpur, Malaysia*
[c] *Department of Chemical Engineering, Universiti Teknologi Malaysia, 81310 Johor Bahru, Malaysia*
[d] *Chemical Engineering Department, Universiti Teknologi Petronas, 32610 Seri Iskandar, Perak, Malaysia*
[e] *Radiation Processing Technology Division, Malaysian Nuclear Agency, 4300 Kajang, Selangor, Malaysia*

Received 27 December 2017; accepted 20 May 2018
Available online 29 May 2018

KEYWORDS

Acidic ionic liquid;
Proton exchange membrane;
Radiation induced grafting;
Fuel cells

Abstract In this study, we proposed an innovative and versatile method for preparation of highly stable and conductive supported ionic liquid (IL) membranes for proton exchange fuel cell applications. Novel covalently supported dual acidic IL membranes were prepared by radiation induced grafting of 4-vinyl pyridine (4-VP) onto poly(ethylene-*co*-tetrafluoroethylene) (ETFE) film followed by post-functionalization via sequential treatments with 1,4-butane sultone and sulfuric acid to introduce pyridinium alkyl sulfonate/hydrogen sulfate moieties. The advantage of our approach lies in grafting polymers with highly reactive functional groups suitable for efficient post-sulfonation. The membranes displayed better swelling and mechanical properties compared to Nafion 112 despite having more than 3 times higher ion exchange capacity (IEC). The proton conductivity reached superior values to Nafion above 80 °C. Particularly, the membrane with ion exchange capacity of 3.41 displayed a proton conductivity of 259 $mScm^{-1}$ at 95 °C. This desired conductivity value is attributed to the high IEC of the membranes as well as dissociation of the hydrophobic

* Corresponding authors at: Advanced Materials Research Group, Center of Hydrogen Energy, Institute of Future Energy, Universiti Teknologi Malaysia, 54100 Kuala Lumpur, Malaysia.
E-mail addresses: ebrahim@utm.my (E. Abouzari-Lotf), mohamed.nasef@utp.edu.my (M.M. Nasef).
Peer review under responsibility of King Saud University.

Production and hosting by Elsevier

https://doi.org/10.1016/j.arabjc.2018.05.010

ETFE polymer and hydrophilic pyridinium alkyl sulfonate groups. Such appealing properties make the supported IL membranes promising for proton exchange membrane fuel cells (PEMFC).

1. Introduction

The growing concerns over depletion of fossil fuels and the drastic climate changes related to its consumption continue to draw an ever-increasing attention towards the development of alternative electrochemical energy technologies (Gold, 2017). In this regard, fuel cells are being considered as one of the most promising green and effectual energy conversion devices (Schultz, 2003; Zhu et al., 2008). Among fuel cell types, PEMFCs are the most promising and attractive candidate for a wide variety of power applications ranging from portable and mobile applications to stationary power systems (Hu et al., 2017; Miyake and Miyatake, 2017; Quartarone et al., 2017). Proton exchange membranes (PEMs) plays a crucial role in PEMFC operation and thus it must have high proton conductivity and excellent mechanical strength in addition to chemical stability. Currently, perfluoronated sulfonic acid membranes such as Nafion® are the most widely used material in PEMFC membranes and display good performance at temperatures $\leq$80 °C (Abouzari-lotf et al., 2017b; Zhang et al., 2012). However, these membranes are challenged by limited operation temperature and high fuel crossover when using liquid fuels (e.g. methanol) in addition to high cost (Abouzari-Lotf et al., 2018; Kim et al., 2015; Tan et al., 2010). Thus, the interest in developing new alternative durable and cost-effective PEMs has been fast growing to prompt the mass deployment of PEMFC technology in the market place (Chen et al., 2018; Gong et al., 2017; Zhang et al., 2015, 2017).

Various ionomeric materials such as modified Nafion, partially fluorinated and non-fluorinated hydrocarbon, acid-doped polymers, inorganic/organic nano-hybrids, solid acids with super-protonic phase transition, and acid/base membranes have been intensively investigated (Abouzari-lotf et al., 2016; Abouzari-Lotf et al., 2016; Assumma et al., 2015; Gubler, 2014; Jothi and Dharmalingam, 2014; Kim et al., 2010; Nasef et al., 2017, 2016; Su et al., 2013). However, most of these membranes are far from meeting the full requirements of high conductivity and stability under fuel cell operating conditions and are mainly challenged by degradation especially over 80 °C (Madden et al., 2010; Nasef, 2014).

Recently, ILs with high ionic conductivity, wide electrochemical stability, negligible vapour pressure and good thermal and chemical stability have been employed for preparation of fuel cell membranes (Che et al., 2015b; Diaz et al., 2014; Fang et al., 2015; MacFarlane et al., 2014; Wang et al., 2016; Yasuda et al., 2012). Among various ILs, protonic ones having mobile protons located on cations showed high conductivity and were proposed as electrolytes in fuel cell applications (Fernicola et al., 2006). Particularly, membranes containing -SO_3H functionalized ILs with a hydrogen sulfate counter-anion have exhibited an excellent thermal stability and reasonable proton conductivity (Díaz et al., 2014). Various methods including gelation (Ishioka et al., 2014; Kataoka et al., 2015), impregnation of porous substrates with ILs (Guerreiro da Trindade et al., 2016; Sekhon et al., 2006), polymerization of ILs (Mecerreyes, 2011; Rhoades et al., 2016) and grafting (Uragami et al., 2016; Zhuo et al., 2015) have been utilized to incorporate ILs in polymer substrates. ILs immobilization on substrates can be carried out either physically or covalently with methods such as self-assembly and polymerisation (Kim and Chi, 2004; Kurane et al., 2013; Valkenberg et al., 2002). In comparison, the covalent immobilization of ILs is advantageous not only in terms of absence of leaching and lower ILs consumption but also because of improvement in stability, reduction of environmental impact and enhancement of membrane economy (Park et al., 2006; Xin and Hao, 2014). Despite various research efforts on ILs-based ionomers (Osada et al., 2016; Ye et al., 2013), the mechanical and chemical stability of the membranes are not satisfactory and there is a strong needs to enhance the stability of membranes without compromising proton conductivity.

In the current approach, in order to design highly conductive and stable ILs based membranes; covalent grafting of dual acidic ILs (pyridinium alkyl sulfonate/hydrogen sulfate) onto poly(ethylene-alt-tetrafluoroethylene) (ETFE) film has been proposed, as shown in the Fig. 1. Due to exclusive combination of mechanical and chemical properties, ETFE has been widely considered a base film for diverse applications including membranes for PEMFC (Güler et al., 2018; Ponce-González et al., 2016; Sproll et al., 2018; Zakeri et al., 2018). Due to grafting onto the highly hydrophobic and stable dense film, IL membranes were expected to be dimensionally stable. On the other hand, introducing of dual acidic groups can directly enhance the ion exchange capacity (IEC) of membranes with slight mechanical stability scarifying upon increasing IEC. The membranes were prepared using graft copolymerisation of 4-VP on ETFE film using radiation induced method followed by chemical immobilization of $[-(CH_2)_4\text{-}SO_3H]HSO_4$ in a 2-step treatment with 1,4-butane sultone and sulfuric acid. The method was flexible in controlling the density of loaded IL. The properties of the obtained membranes were investigated using Fourier transform infrared (FTIR), scanning electron microscopy (SEM), dispersive X-ray spectroscopy (EDS), X-ray photoelectron spectroscopy (XPS), X-ray diffraction (XRD), thermal gravimetric analysis (TGA), differential scanning calorimetry (DSC and thermomechanical analysis (TMA). Other significant properties such as water uptake, ion exchange capacity, ionic conductivity and chemical and dimensional stability were also evaluated.

2. Experimental

2.1. Materials and methods

Melt-processed semi-crystalline ETFE film with thickness of 50 μm were commercially obtained from Good fellow (Cambridge, England). The dense film is highly hydrophobic with

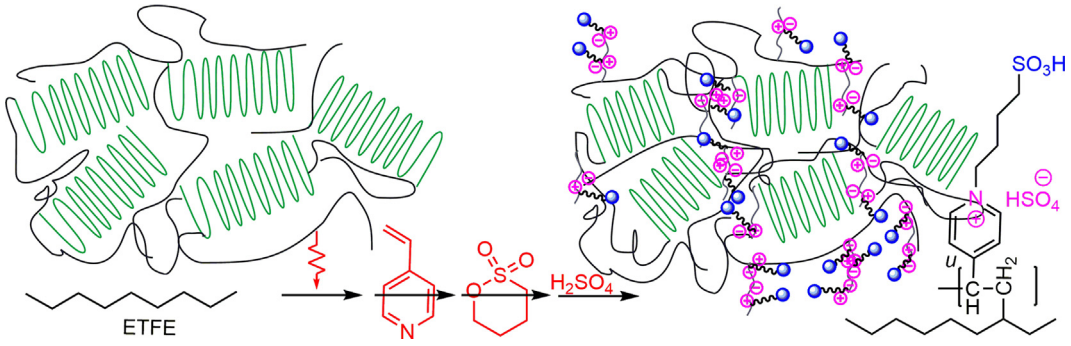

Fig. 1 Schematic representation of the preparation of supported dual acidic ionic liquids.

water permeability of 170×10^{-13} $cm^3 \cdot cm\ cm^{-2}\ s^{-1}\ Pa^{-1}$ at 38 °C. 4-VP (>95% purity) and 1,4-butane sultone (≥99% purity) were purchased from Aldrich and used without any further purification. Acetonitrile was pre-dried by shaking over type 4 Å molecular sieve particles followed by distillation over calcium hydride. Other chemicals including iron (II) sulfate, sulfuric acid, hydrogen peroxide, hydrochloric acid and potassium hydroxide were analytical grade and used as received. Deionised (DI) water (18 MΩ resistivity) was used in all experiments and was produced using a NANO pure DIamond™ water purifier.

2.2. Preparation of poly(4-VP) grafted ETFE films (membrane precursor)

The poly(4-VP) grafted ETFE films were prepared using pre-irradiation method started by irradiation with electron beam (EB). ETFE films (5 cm × 5 cm) were washed with ethanol and dried under vacuum oven prior to recording their weight and keeping them in thin polyethylene bags sealed under vacuum. The films were irradiated to a total dose of 100 kGy with an EB using a universal accelerator (NHV-Nissin High Voltage, EPS 3000, Cockroft Walton type, Japan) operated at an acceleration voltage of 1 MeV, beam current of 2 mA and 10 kGy dose per pass.

In the second step, grafting of 4-VP onto irradiated ETFE films was performed by introducing O_2 free monomer solution diluted with water obtained by bubbling with purified N_2 gas for 30 min to an evacuated glass ampoule containing the irradiated ETFE film. The ampoule was sealed and heated in a water bath at 60 °C to start the grafting reaction. After the reaction was completed, the grafted film was removed, washed with methanol under sonication for several hours to remove the unreacted monomer and/or homopolymers. The grafted film was dried under vacuum at 60 °C overnight and the weight of the grafted film was determined. The grafted film was denoted as ETFE-*g*-poly(4-VP). The degree of grafting (DOG) was determined from the following equation and confirmed by TGA.

$$DOG\ (\%) = \frac{W_g - W_a}{W_a} \times 100 \quad (1)$$

where W_a and W_g are the weights of the grafted and original ETFE films, respectively.

2.3. Immobilization of IL onto grafted ETFE films

The ETFE-*g*-poly(4-VP) films were treated with 1,4-butane sultone to introduce sulfonic acid alkyl pyridinium IL. The reaction was carried out by immersing the ETFE-*g*-poly(4-VP) films in a dry acetonitrile in two-neck 250 mL round flasks under inert atmosphere. The mixture was cooled to 0 °C in an ice bath and 1,4-butane sultone/acetonitrile 2% (v/v) was added. The mixture was heated to 85 °C under continuous stirring for two days to obtain the corresponding zwitterion denoted as ETFE-*g*-poly(4-VP)-SO_3 that was washed with diethyl ether (3 × 25 mL) and dried under vacuum. The obtained zwitter ion was then immersed in a 1 M H_2SO_4 solution under stirring for 24 h at 60 °C to obtain supported dual acidic IL [ETFE-*g*-poly(4-VP)-SO_3H]HSO_4 membranes, which were then extracted with deionised water and rinsed in water and ethanol solutions before drying under vacuum at 80 °C for 48 h.

The number of sulfonic acid molecules per alkyl substituted pyridine rings of the grafted matrix or degree of sulfonation was calculated and found to be 50% of the total poly(4-VP) grafted on ETFE films. The reaction was repeated in a higher concentration of the 1,4-butane sultone and longer reaction time to increase the acid functionalization level per polymer repeating unit. A complete sulfonation (i.e., all alkyl pyridine groups in the membranes were fully sulfonated) was achieved with the increase in the 1,4-butane sultone/acetonitrile concentration to 5% (v/v) and the time to 3 days. Membranes with high IEC (ETFE-d-IL3.2 and ETFE-d-IL3.4 with DOG of 46 and 59%, respectively) were chosen for further evaluation of the properties.

2.4. Evolutions of properties of [ETFE-g-poly(4-VP)-SO_3H]HSO_4 membranes

Micrographic images of the obtained membranes were obtained using a Philips XL30 field emission scanning electron microscope (FE-SEM) after coating with 5 nm Au. Energy dispersive X-ray spectroscopy (EDS) was performed with Zeiss GeminiSEM 500. FTIR coupled with attenuated total reflection (FT-IR-ATR) analysis was performed using an Agilent Cary 660 spectrometer. XRD diffraction patterns were obtained by a Philips X'Pert 1 X-ray diffractometer with graphite monochromatised Cu Kα radiation (λ = 1.5401 Å) at a scanning rate of 2° min^{-1} over range of 2θ = 4–80°. X-ray photoelectron spectroscopy (XPS) was performed with PHI

Quantera II Scanning XPS Microprobe with a monochromatic radiation source of Al Kα anode (1486.6 eV) at a pressure $< 1 \times 10^{-8}$ bar at room temperature. Peak integration was carried out followed by deconvolution of the C 1s peaks by assuming a Gaussian line shape. TGA measurements were performed on a Perkin Elmer TGA 7 under N_2 atmosphere in a temperature range of 20–700 °C at a heating rate of 10 °C min^{-1}. The thermal properties of membrane samples were measured by a Perkin Elmer, Pyris-1 DSC. The degree of crystallinity (X_c) has also been calculated from the ratio of enthalpy of melting (ΔH_f) of polymer electrolyte to the enthalpy of melting for a fully crystalline polymer (ΔH_0 = 113.4 Jg^{-1} for ETFE).

$$X_c = \frac{\Delta H_f}{\Delta H_0} \times 100\%$$

TMA measurements were carried out with a TA Instrument 2940 in a tensile film mode using sample dimensions of 20 mm × 5 mm × 0.075 mm under N_2 atmosphere. The experiments were run at a temperature ranging from 30 to 350 °C with a temperature ramp rate of 5 °C min^{-1}.

IEC was determined by the back-titration method. The membrane in the acid form was immersed in 50 mL of deionized water containing 5 mL of 0.1 N NaOH for 48 h in order to release H^+. The back-titration was accomplished by titrating the excessive NaOH remaining in solution with 0.1 M HCl solution. The IEC value was obtained by subtracting the added volume of 0.1 M HCl from the initial NaOH volume. Each data point of IEC measurements reported is an average of three measurements. Mohr titration method was used to determine Cl^- per g of dried membrane samples as reported elsewhere (Abouzari-lotf et al., 2017a).

In-plane ionic conductivity of the membranes was measured using DC source meter (Keithley 2400 from Keithley Instruments Inc., Cleveland, OH, USA) attached to a four-point probe of Bekk-Tech conductivity cell (BT-112) and controlled by a Lab view software. Membrane strips with dimensions of 5 mm × 25 mm were assembled between the platinum electrodes and placed in conductivity cell. The potentiostat was set to apply a specific voltage between the two inner probes and measured the resulting current. The slope of the data from current versus voltage measurements was applied to determine the resistance (R) and proton conductivity (σ) obtained according to the following equation:

$$\sigma\ (\mathrm{S/cm}) = \frac{d\ (\mathrm{cm})}{R\ (\Omega) \times A\ (\mathrm{cm})^2} \tag{2}$$

where d and A are the thickness and surface area of the sample, respectively. The thickness of the membrane was determined from SEM cross-sectional image.

The water uptake and swelling of the membranes were obtained by recording the changes in the weights and dimensions. The membrane samples were dried under high vacuum for 24 h and weighed prior to equilibrate in de-ionised water for 24 h at various temperature. The samples were then taken out, blotted dry and the weights and dimensions were quickly measured. The gravimetric water uptake was calculated using the following equation:

$$\emptyset_w = \frac{W_{wet} - W_{dry}}{W_{dry}} \times 100 \tag{3}$$

where W_{wet} is the weight of the membrane after soaking in water for 24 h and W_{dry} is the weight after drying under a high vacuum for 24 h.

In the same way, the swelling in-plane (S_{in}) and through-plane (S_{tr}) of the membranes in de-ionised water were calculated using the following equation:

$$S_x = \frac{X_{wet} - X_{dry}}{X_{dry}} \times 100 \tag{4}$$

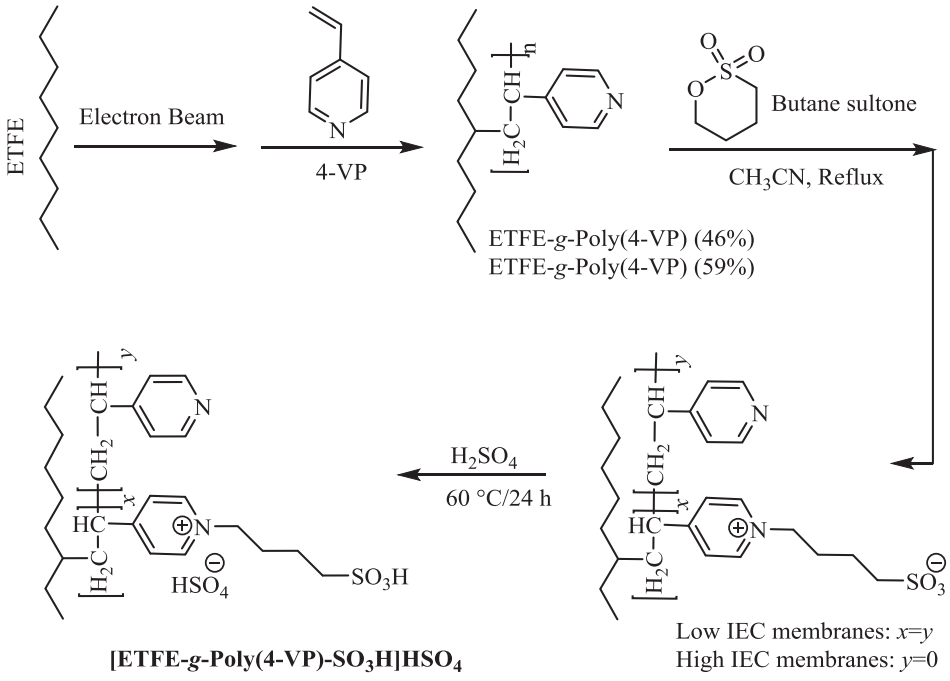

Fig. 2 Schematic representation for preparation of supported dual acidic IL membranes.

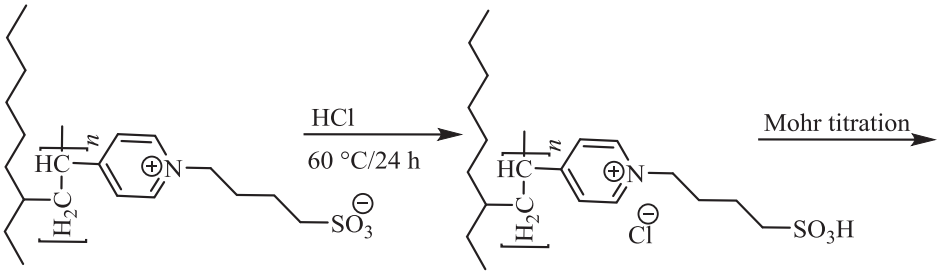

Fig. 3 Schematic representation for preparation of supported dual acidic IL membranes with Cl^- counter ion.

where S_x represents desired swelling (S_{in} or S_{tr}) based on corresponding changes in dimensions or thicknesses in swollen (X_{wet}) and dry (X_{dry}) membranes, respectively.

The chemical stability of the membranes was evaluated by Fenton agent containing 3% H_2O_2 and 2 ppm $FeSO_4$. Preweighed dry membranes were soaked in a Fenton aqueous solution at 30 °C for periods up to 120 h and the stability was evaluated by recording the weight retained in the membranes after complete drying. The ability of the membranes to retain their ionic character (i.e. durability) was tested by evaluating the proton conductivity under different time intervals up to 120 min.

3. Results and discussion

The IL supported membranes were prepared in 4 steps involving irradiation of ETFE films with EB, grafting of irradiated ETFE with 4-VP, treatment of the grafted films with 1,4-butane sultone and sulfuric acid. Fig. 2 shows a schematic representation for preparation of the supported dual acidic IL membranes obtained in this study.

To further confirm the formation of dual acidic groups, the obtained zwitter ion was acidified with hydrochloric acid and amount of Cl^- per g of dried polymer was determined via the Mohr titration method, as shown in the Fig. 3.

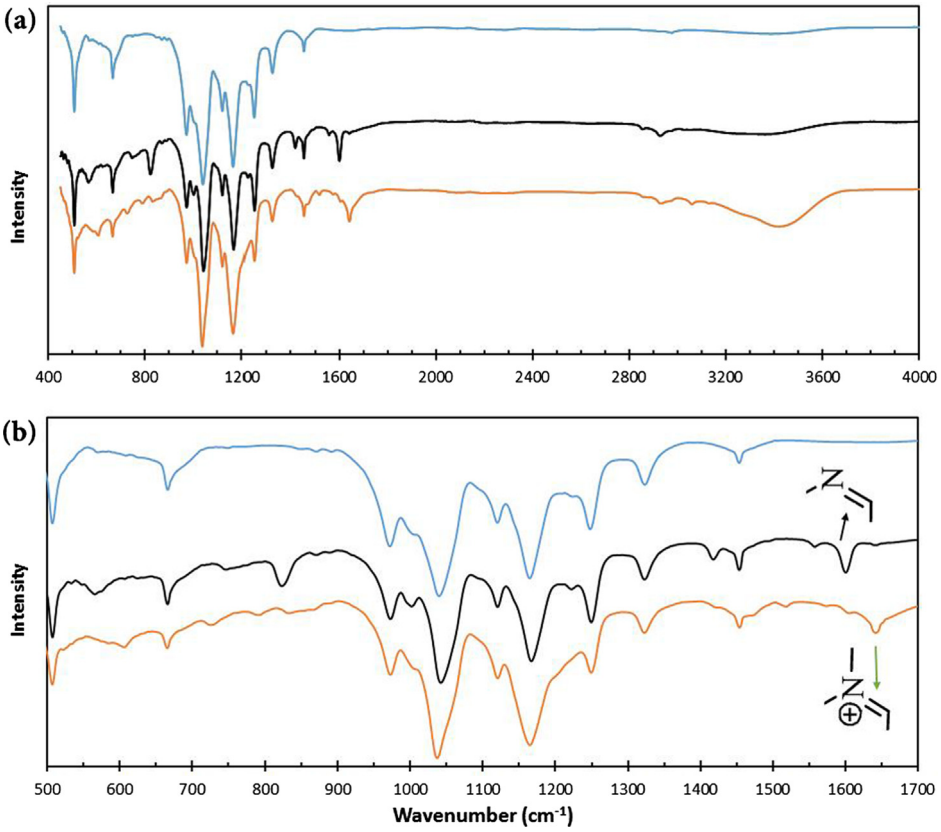

Fig. 4 FTIR spectra of (a) original ETFE film (blue), ETFE-*g*-poly(4-VP) film with 46% DOG (black) and corresponding supported IL membrane (red) and (b) expanded IR spectra in the region of 500–1700 cm^{-1}. (For interpretation of the references to colour in this figure legend, the reader is referred to the web version of this article.)

3.1. Chemical composition of the membranes

FT-IR spectra in Fig. 4 shows the characteristic absorption bands of ETFE based ionic liquid electrolyte membrane in comparison with their corresponding poly(4-VP) grafted and original ETFE film. The spectrum of original ETFE film is identified by the presence of a number of strong bands in the range of 1000–1400 cm^{-1} representing C—F of CF_2 groups. The grafted films displayed characteristic bands representing C═N and C═C of pyridine ring stretching vibrations at 1600, 1558, and 1418 cm^{-1}. The bands in the range of 720–850 cm^{-1} is related to C—H bending of pyridine ring. The [ETFE-g-poly(4-VP)-SO_3H]HSO_4 membrane showed a abroad band at 3200–3600 cm^{-1} region, which is associated with —OH stretching vibration of the sulfonic acid group in the membrane. Moreover, the quaternary salt of pyridinium in IL immobilized ETFE showed a band at 1640 cm^{-1}. This band can be assigned to C═N vibrations characteristic of the quaternary nitrogen atom in the pyridine ring.

To further elucidate the chemical structure and uniform ILs functionalization at the surface and core of ETFE substrates, XPS and EDS analysis were applied on the membrane surface and cross-section, respectively. Both techniques are highly sensitive to the surface with few nanometers of attenuation depths. Fig. 5 shows a survey scan and high-resolution narrow scans of C 1s and S 2s spectra. Compared to the two peaks in C 1s spectra of pristine ETFE at 286.0 eV (due to —CH_2—) and 290.5 eV (due to —CF_2—), (Gajos et al., 2016; Yamamoto et al., 2008), C 1s of IL functionalized ETFE was deconvoluted into 9 peaks corresponding to different C atoms in the structure of IL loaded membrane. They include aromatic and aliphatic —CH_2— (C—C^*—C) at 284.5 eV, main chain —CH_2— at 286.0 eV, C—S at 287.2 eV, C═N^+ at 288.4 eV, C—N^+ at 289.3 eV, grafted IL units onto —CF— at 290.5 eV, main chain —CF_2— at 290.8 eV, and two peaks at higher binding energy of 292.2 and 293.1 eV which are likely to be due to the shake-up satellites of carbons or possible changes (e.g. crosslinking and unsaturation) in the ETFE backbones upon irradiation.

The chemical composition and uniformity of membranes were further confirmed with EDS analysis of surface and cross-section and the obtained images are presented in Fig. 6. The membrane was proven to contain elemental oxygen, sulfur and fluorine. Moreover, mapping of such elements confirms the presence of a uniform distribution of ionic liquid groups in the membrane surface and cross-section. These observations clearly confirm that the incorporation of poly (4-VP) grafts providing the host for ionic liquid took place homogenously across the membrane during the grafting reaction.

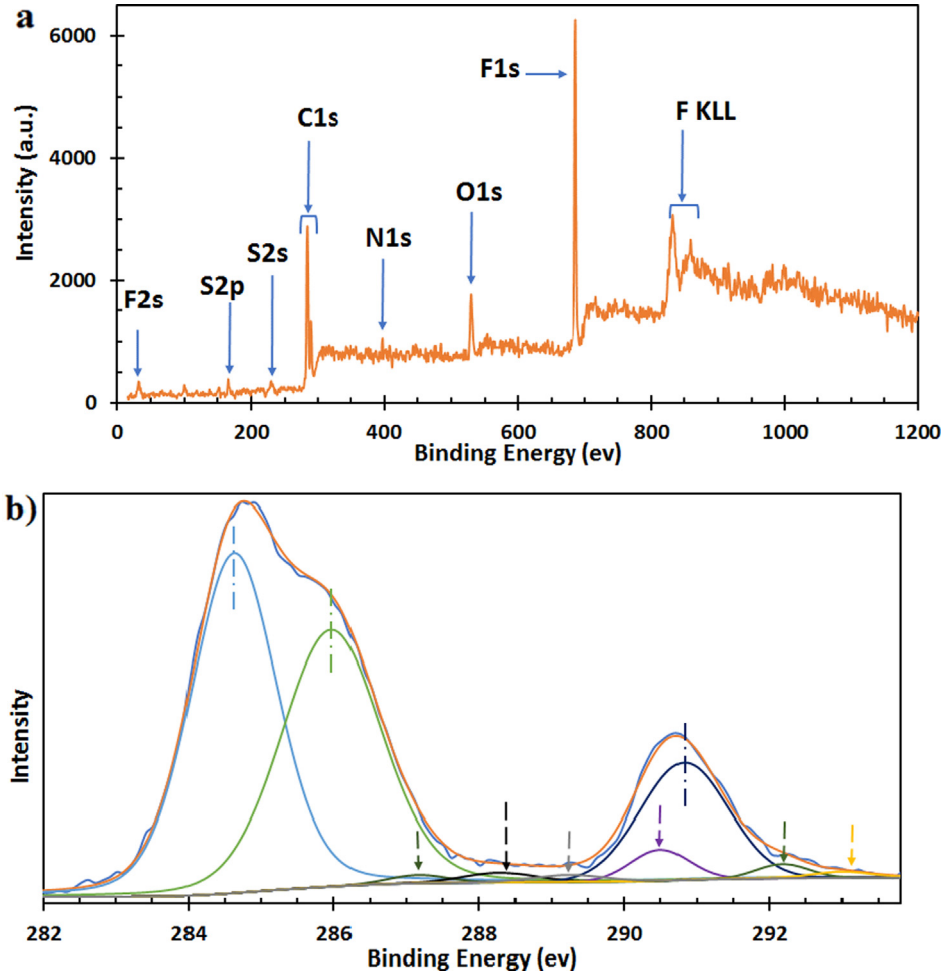

Fig. 5 XPS spectra: wide scan (a) and narrow scan with deconvoluted C 1s peaks (b) of supported IL membrane.

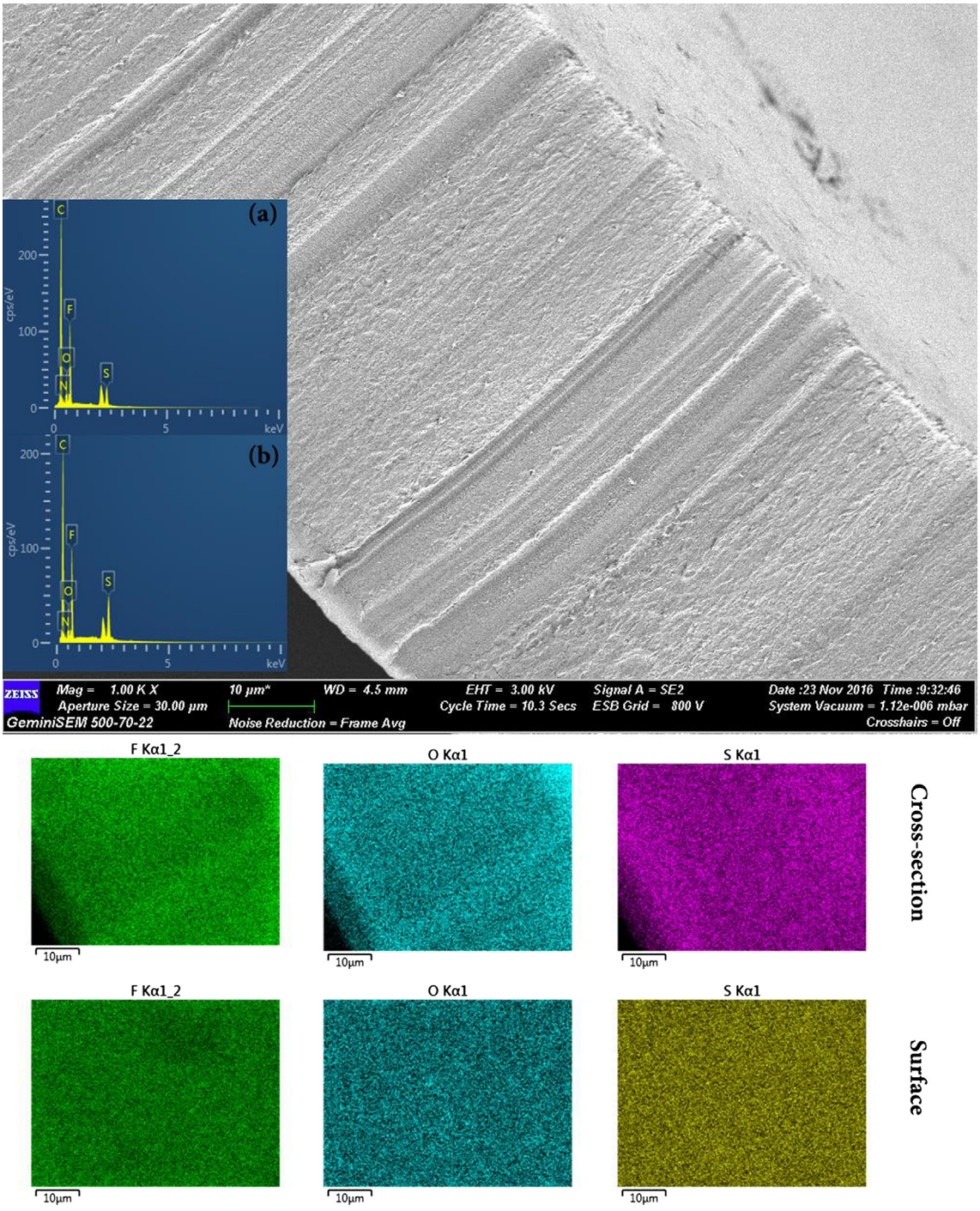

Fig. 6 SEM images of membrane with 46% DOG: cross-section (top) and membrane EDX mapping with analysis of F, O, and S atoms of cross-section and surface views (bottom).

3.2. Morphology of the membranes

The SEM images of the original ETFE, grafted and IL immobilized ETFE films are shown in Fig. 7. It was found that ETFE control membrane (Fig. 7a) was dense, uniform and defect free. The surface morphology of the grafted ETFE film (Fig. 7b) displayed white dots which represent 4-VP uniformly distributed on the surface of the polymer matrix. Upon incorporation of ILs in the membrane, numerous short-rang and roomy channels can be clearly distinguished in the image of supported IL membrane (bright colour in Fig. 7c), which can be attributed to the aggregation of ILs within the formed ionic clusters. In fact, these irregular channels emerged as a result of the dissociation of the hydrophobic ETFE polymer and hydrophilic pyridinium alkyl sulfonate groups (Che et al., 2015a; Wu et al., 2016).

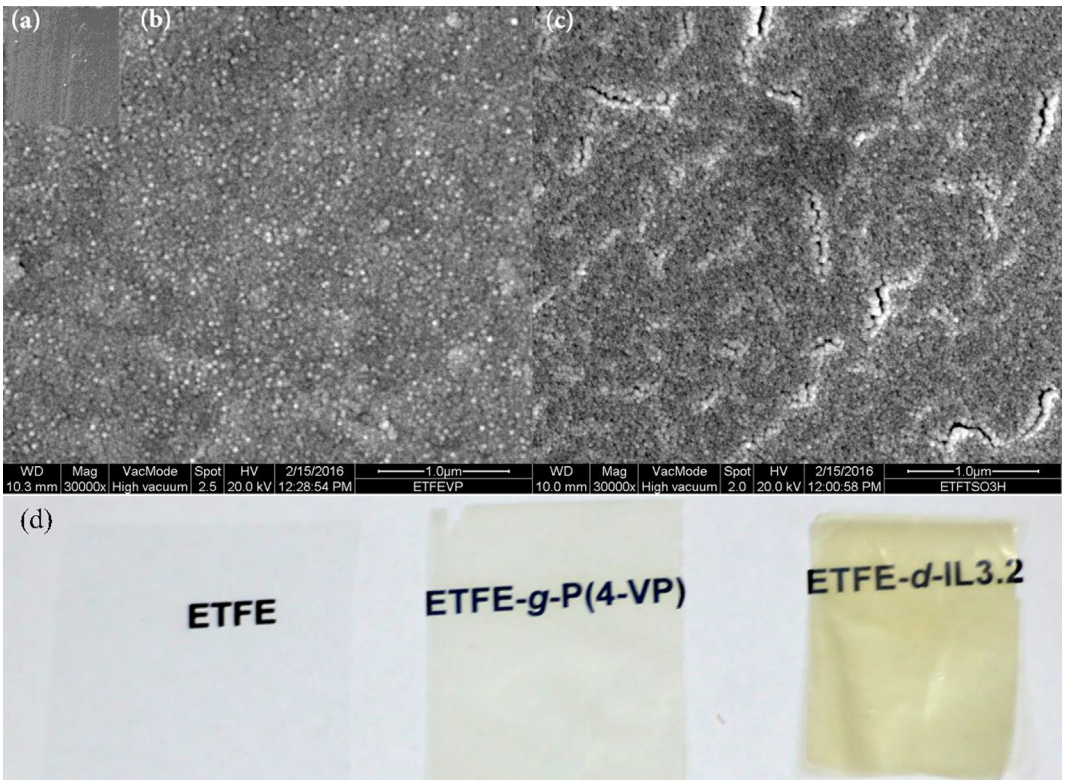

Fig. 7 SEM images of (a) original ETFE film, (b) ETFE-*g*-poly(4-VP) film with 46% DOG and (c) supported IL membrane and related photographs (d).

3.3. Thermal properties of the membranes

Fig. 8a shows TGA thermograms of original ETFE film, poly (4-VP) grafted film and supported IL membrane. The original ETFE film shows a single-step degradation pattern starting at 440 °C while ETFE-*g*-poly(4-VP) film exhibits a two-step degradation pattern. The first step represents the decomposition of poly(4-VP) grafts started at 320 °C and the second one began at 440 °C is assigned for the decomposition of ETFE backbone. Interestingly, the exact value of DOG could be also calculated from the TGA thermograms of grafted films. Typically, the DOG value for this sample was found to be around 43%, which is in good agreement with the calculated data based on the gravimetric changes. For [ETFE-*g*-poly(4-VP)-SO_3H]HSO_4 film, three-step degradation pattern was observed at temperatures of 280, 320 and 440 °C. The first weight loss at around 280 °C belongs to the decomposition of butyl sulfonic acid groups, whereas the second and third steps (320 and 440 °C) are due to the decomposition of grafted poly (4-VP) and ETFE backbone, respectively. The observed weight loss that started at a temperature below 100 °C and continues to 150 °C in the grafted film and IL membrane is due to the loss of water molecules involved in hydrogen bonds. From the TGA results, it can be concluded that supported IL membranes have a thermal stability suitable for PEMFC operation at high temperature (> 100 °C).

Fig. 8b shows DSC thermograms of the supported IL membrane and their corresponding grafted and original ETFE films. The strong endothermic peak at 269 °C depicts the melting temperature (T_m) and the area under the peak represents the crystalline fraction of the original ETFE film. Grafting of poly(4-VP) shifted T_m to 265 °C and decreased the total area under the melting peak suggesting a reduction in the crystalline fraction of the ETFE. This is caused by the dilution of the crystalline phase with the incorporation of amorphous poly (4-VP) grafts. The reduction of melting peak area caused by incorporation of IL results a partial disruption along with the plasticization effect of IL which conforms the increase in the amorphous phase. This observation is going well with the calculated X_c, which showed a reduction from 36.5% in the original ETFE film to 26.2% and 25.1% in the grafted film and supported IL membranes, respectively. Nevertheless, the membrane maintains a reasonable level of X_c despite the dilution effect and minor disruption in its crystalline structure.

The thermomechanical behaviour of the original ETFE, grafted ETFE film and supported IL membrane was examined by TMA to determine the T_g as shown in Fig. 8c. The TMA thermograms showed that there is a decrease in T_g of the supported IL membrane compared to those of the original and the grafted ETFE films. Such decrease was expected as the T_g of a polymer is directly related with the mobility of polymeric chains.

3.4. Structural properties of the membranes

X-ray diffraction measurements were carried out to monitor the structural changes took place in the ETFE matrix by the incorporation of poly(4-VP) grafts and subsequent IL grafted ETFE as depicted in curves presented in Fig. 9. The original ETFE film shows a typical diffraction curve resembling a semicrystalline polymer with a crystalline fraction peak at 19.6° and amorphous halo at 40.2°. The XRD curve of the grafted ETFE film shows a similar crystallinity peak but with

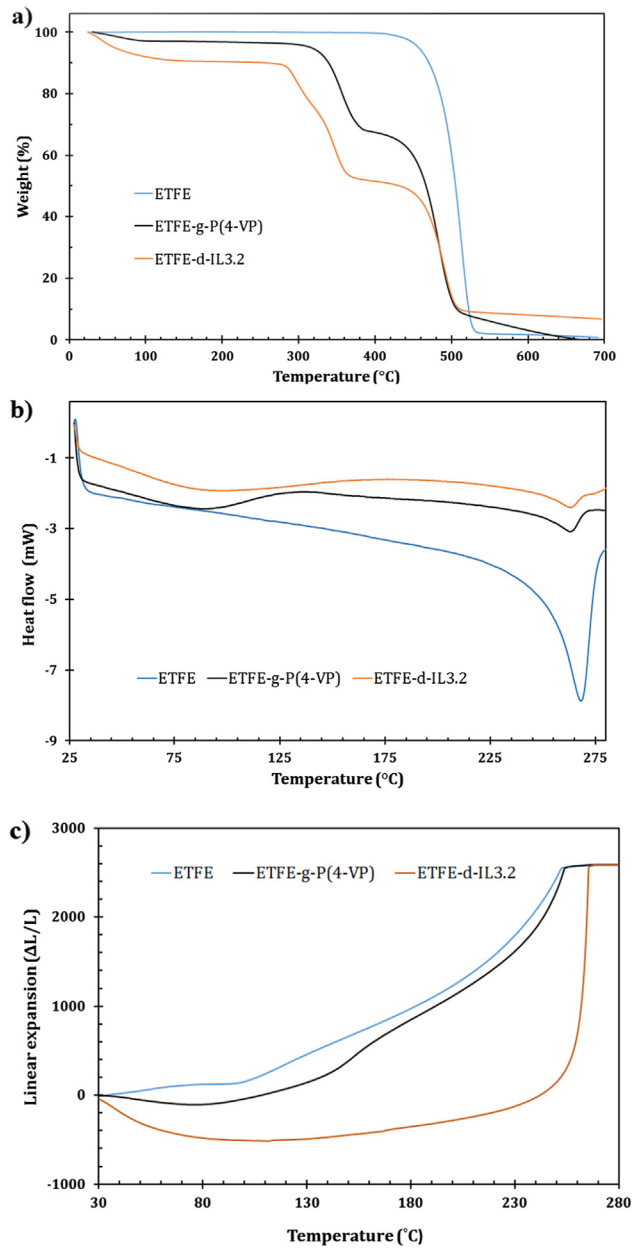

Fig. 8 TGA (a), DSC (b) and TMA (c) thermograms of original ETFE film, ETFE-*g*-poly(4-VP) film with 46% DOG, and corresponding supported IL membrane.

a reduced intensity without any obvious shift in the crystalline peak position. This indicates that there is a decrease in the degree of crystallinity under the influence of dilution effect caused by incorporation of the amorphous poly(4-VP) grafts in the polymer matrix. It can be seen that IL grafted ETFE film consists of less intense and broader halos. The broadening of the peaks and reduction in intensity of crystalline phase is due to increase in amorphicity of polymeric membrane caused by the plasticization effect of IL.

3.5. IEC, water uptake, dimensional stability of the membranes

The values of IEC of the membranes are presented in Table 1. The IEC increased from 3.20 (in ETFE-d-IL3.2 membrane) to 3.41 mequiv g^{-1} (in ETFE-d-IL3.4 membrane) with the rise in DOG from 46 in the former to 59% in the latter. This observation can be attributed to the increase in the content of poly(4-VP) grafts that can host more sulfonic acid groups. The IEC values of the new membranes are almost 3 times higher than that of Nafion 112 and this is likely due to the presence of large number of dual ionic linkage in their molecular structure. On the other hand, Mohr titration method resulted in the values which are almost half of the IEC values which clearly confirms the presence of dual acidic groups.

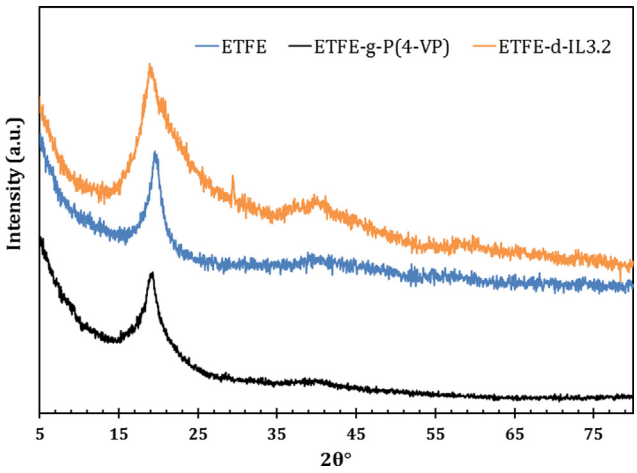

Fig. 9 XRD curves of original ETFE film, ETFE-*g*-poly(4-VP) with 46% DOG and supported IL membrane.

The water uptake and swelling are two important parameters for PEMs, which represent their water retention and dimensional stability, respectively. According to the vehicle mechanism of proton transport, an appropriate amount of water content in PEMs is necessary for achieving high proton. On the other hand, excessive water content in membranes could deteriorate dimensional stability and even results in serious loss of mechanical properties (Kreuer, 2001). Therefore, a promising PEM should balance the two properties and thus achieved high proton conductivity as well as excellent dimensional stability. The water uptake and swelling were measured at the temperatures ranging 30 and 80 °C and the results are displayed in Table 1. Compared to the negligible water uptake values for the pristine ETFE film, IL functionalized membranes showed significant interaction with the water due to the inclusion of hydrophilic ionic groups. As shown, for the IL membranes, the water uptake increased with sulfonation degree and temperature. On the other hand, ETFE-d-IL3.4 showed the higher water uptake than that of ETFE-d-IL3.2 at the same temperature due to higher content of sulfonic acid groups.

The dimensional changes associated with water swelling in the supported IL membranes and Nafion 112 at 30 and 80 °C are also presented in Table 1. All the membranes demonstrated increased swelling ratios with the temperature increase. However, the swelling ratio of the supported membranes were interestingly lower than that of Nafion despite their higher IECs. In addition to the inherent stability of base ETFE film, it seems that the grafted dual acidic ILs have restricted volumetric expansion during swelling which favours a higher IEC.

Table 1 IEC, water uptake and dimensional stability of IL immobilized membranes in comparison with Nafion 112.

Samples	IEC	Water uptake (%)			Dimensional changes at 30 °C[a]		Dimensional changes at 80 °C[a]	
	(mequiv g^{-1})	30 °C	70 °C	80 °C	S_{in}	S_{tr}	S_{in}	S_{tr}
ETFE-d-IL3.2	3.20	7.8	10.8	15.2	2.8	6.6	8.6	12.3
ETFE-d-IL3.4	3.41	8.3	11.3	16.1	3.1	8.2	9.2	13.9
Nafion 112	0.91	33.0	35.4	38.1	9.3	9.0	–	–

[a] In-plane (S_{in}) and through-plane (S_{tr}) of membranes after soaking in water at 30 and 80 °C for 24 h.

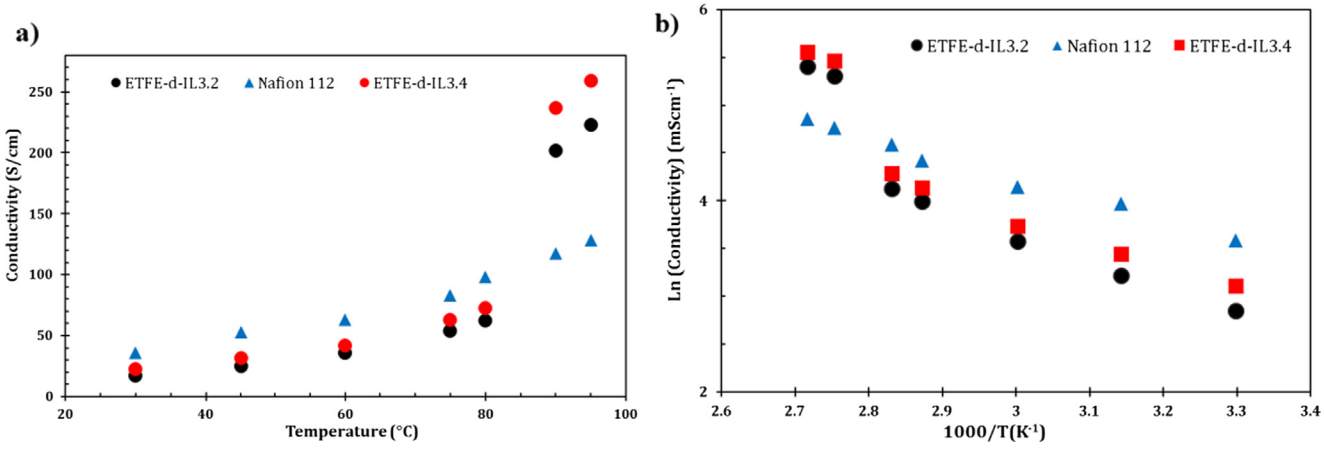

Fig. 10 Variation of proton conductivity of: (a) supported IL membranes and Nafion 112 with temperature and (b) the corresponding Arrhenius plots.

3.6. Proton conductivity of the membranes

Fig. 10a shows the variation of proton conductivity with the temperature for two supported IL membranes and Nafion 112 at 100% relative humidity. The proton conductivity showed a temperature dependant trend in all membranes. However, the increasing of conductivity with temperature was rather continuous in Nafion 112 membrane throughout the temperature range (30–95 °C) whereas it took place in two consecutive stages in the supported IL membranes. For instance, the increase in conductivity of both IL membranes was lower than that of Nafion 112 in the temperature range of 30–80 °C (first stage) beyond which (second stage) it jumped to greater values reaching 223 mS cm^{-1} for ETFE-d-IL3.2 and 259 mS cm^{-1} for ETFE-d-IL3.4 at 80–95 °C compared to 160 mS cm^{-1} for Nafion 112 membrane at the same temperature. Such interesting temperature-dependent conductivity trend can be attributed to the mobile protons produced in the dissociation of HSO_3 groups. The polymeric membranes are formed by pyridinium cations with sulfonic groups as side chains and HSO_3^- anions that is essentially a strong acid. Thus, when exposed to water and temperature, the sulfonate groups present in both counter-ions dissociate into SO_3^- and free mobile protons (Kataoka et al., 2015). As TGA thermogram showed, these supported membranes contain high amounts of retained water inside their chemical structure, there are plenty of mobile protons that can easily jump through the H-bonded network formed by ions and water molecules (Wojnarowska et al., 2014). On the other hand, it looks like that the jumping in conductivity values between 80 and 95 °C is due to some kind of phase transition. Since water uptake values also changes intensely at this temperature window (comparing the values for 70 and 80 °C in Table 1), it could be concluded that the transition is from crystalline to amorphous.

The dependence of the proton conductivity of the membranes on the temperature (T) was investigated and the data were fitted to Arrhenius equation given below:

$$\ln(\sigma) = -\frac{E_a}{R}\left(\frac{1}{T}\right) + \ln\sigma_0$$

where σ is the proton conductivity, σ_0 is the pre-exponential factor (mS/Kcm), E_a is the activation energy, T is the temperature in K and R is the universal gas constant (8.314 J mol^{-1} K^{-1}). The obtained data were plotted in Fig. 10b in which 2-region linear trends were observed for both IL membranes resembling a similar trend to that discussed in Fig. 10a. In the first region where the temperature increased from 30 to 80 °C, the data were fitted to a straight line suggesting a proton hopping mechanism in association with high protons and alkyl chains mobilities. In the region above 80 °C, the ionic conductivity increased sharply reaching approximately four times higher values than lower temperature while maintaining a linear trend up to 95 °C. The facilitated mobility of proton hopping sites within membrane due to the phase transition could be the main factor for this increase. This was evident from the lower activation energy (E_a) of the two IL membranes recorded at the temperature range of 80–95 °C (E_a = 18.6 and 21.4 kJ mol^{-1}) compared to that for the range 30–80 °C (E_a = 19.6 and 22.1 kJ mol^{-1} for membranes I and II respectively). These observations suggest that the supported IL

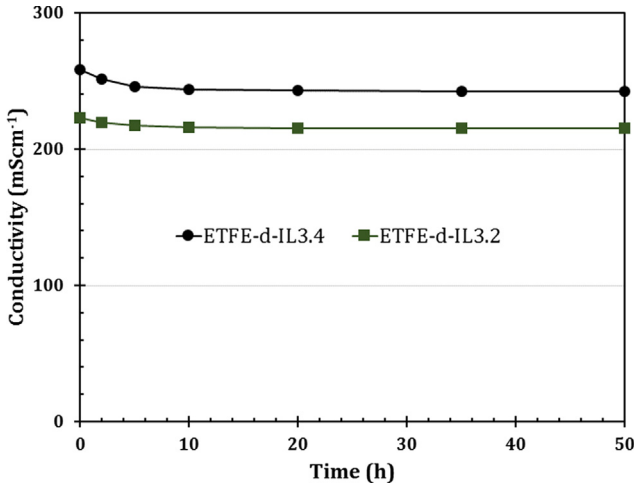

Fig. 11 Variation of proton conductivity of supported IL membranes with time.

membranes obtained in this study possess high proton conductivity suitable for operating PEMFC above 80 °C.

The stability of proton conductivity of the developed membranes was evaluated in a fully hydrated state at 95 °C over a period of 50 h and the obtained data was plotted in Fig. 11. The prolonged proton conductivity in the two supported IL membranes was found to slightly decrease yet remained stable over a period of 50 h. For instance, the conductivity slightly decreased from 259 to 242 mS cm^{-1} in ETFE-d-IL3.4 and from 223 to 215 mS cm^{-1} in ETFE-d-IL3.2 after 5 h and remained unvaried for 50 h. This trend indicates that the supported dual acidic IL membranes are stable enough for future testing in PEMFC.

3.7. Chemical stability of the membranes

The accelerated oxidative degradation test of supported IL membranes was investigated in Fenton's reagent (3% H_2O_2 aqueous solution containing 2 ppm $FeSO_4$) at 30 °C and the obtained data are presented in Table 2. It was interestingly found that only 1 and 4% weight losses could be observed in both supported IL membranes after 5 h compared to ~9% weight loss in Nafion 112 under same conditions. Since the pristine ETFE was stable in the similar test condition, it could be concluded that degradations in the first 5 h were mainly occurring in the grafted regions. Prolonging the time to 24 and 48 h led to equivalent weight losses in all membranes reaching about 10 and 15%, respectively. Comparing to the initial degradations in the pristine ETFE, weight losses after 24 and 48 h could be arising from degradations in both of the grafted regions and ETFE backbone. Nevertheless, the supported IL membranes retained their physical properties such as flexibility and transparency and resisted dissolution in Fenton's reagent after 120 h period as Nafion 112. These results suggest that supported IL membranes obtained in this study have desired high chemical stability. Such enhanced chemical stability can be attributed to the durable ETFE backbone with covalently grafted pyridine ring and covalently immobilization of ionic groups in the membrane.

4. Conclusions

New stable supported dual protic IL membranes [ETFE-*g*-poly(4-VP)-SO_3H]HSO_4 with different DOG were successfully prepared by covalent immobilization of IL onto basic films obtained by radiation induced grafting of 4-VP onto ETFE film followed by sulfonation with 1,4-butane sultone and sulfuric acid treatments. The incorporation of ILs groups and their uniform distribution across the dense ETFE film were confirmed. The IEC of the membranes increased with the increase in the DOG. The proton conductivity was found to be temperature and IEC- dependent. The membrane having an IEC of 3.41 mequiv g^{-1} showed a proton conductivity of 259 mS cm^{-1} in a full hydrate state at 95 °C, which is far higher than that of Nafion 112 (160 mS cm^{-1}) under the same conditions. The IL membranes exhibited lower water uptake and higher dimensional stability than Nafion 112 membrane. Moreover, the membranes showed an outstanding chemical stability in a strong oxidative environment (Fenton's reagent) as indicated by the negligible weight loss in the membrane after 5 h and its remaining undissolved over a period of 120 h. Moreover, the proton conductivity remained stable over a period of 50 h. The membrane extraordinarily maintained high structural stability represented by the crystallinity rise despite the multistep procedure used in preparation. The thermomechanical and thermogravimetric analysis showed that supported IL membranes have excellent thermal and dimensional stability. Finally, the overall ex-situ evaluation of the properties suggests that these IL supported membranes are promising candidates for PEMFC application.

Acknowledgement

This research was funded by the Research University Fund Scheme, Universiti Teknologi Malaysia (grant number # 17H21); and Malaysian Ministry of Higher Education (MOHE) FRGS fund (grant number # 4F878). M. Zakeri and M. Miyake are thankful for the financial support from

Table 2 Chemical stability parameters of membrane dissolution and remaining weight (RW) after 1, 5, 24 and 48 h in Fenton's reagent at 30 °C.

Samples	Thickness (μm)	RW_{1h} (wt%)	RW_{5h} (wt%)	RW_{24h} (wt%)	RW_{48h} (wt%)	T_{dis}[a] (h)
ETFE	50.0	100	99.9	97.1	94.6	> 120
ETFE-d-IL3.2	60.7	99.1	98.9	91.0	85.1	> 120
ETFE-d-IL3.4	61.4	97.6	96.2	89.9	84.4	> 120
Nafion 112	66.4	97.8	91.4	90.7	84.2	> 120

[a] Dissolution time of membrane in Fenton's reagent.

Malaysia–Japan International Institute of Technology (vote no. #00580).

References

Abouzari-Lotf, E., Etesami, M., Nasef, M.M., 2018. Carbon-based nanocomposite proton exchange membranes for fuel cells. In: Carbon-Based Polymer Nanocomposites for Environmental and Energy Applications. Elsevier, pp. 437–461. 10.1016/B978-0-12-813574-7.00018-6.

Abouzari-Lotf, E., Ghassemi, H., Mehdipour-Ataei, S., Shockravi, A., 2016. Phosphonated polyimides: enhancement of proton conductivity at high temperatures and low humidity. J. Membr. Sci. 516, 74–82. https://doi.org/10.1016/j.memsci.2016.06.009.

Abouzari-lotf, E., Ghassemi, H., Nasef, M.M., Ahmad, A., Zakeri, M., Ting, T.M., Abbasi, A., Mehdipour-Ataei, S., 2017a. Phase separated nanofibrous anion exchange membranes with polycationic side chains. J. Mater. Chem. A 5, 15326–15341. https://doi.org/10.1039/C7TA03967K.

Abouzari-lotf, E., Jacob, M.V., Ghassemi, H., Ahmad, A., Nasef, M. M., Zakeri, M., Mehdipour-Ataei, S., 2016. Enhancement of fuel cell performance with less-water dependent composite membranes having polyoxometalate anchored nanofibrous interlayer. J. Power Sources 326. https://doi.org/10.1016/j.jpowsour.2016.07.027.

Abouzari-lotf, E., Nasef, M.M., Zakeri, M., Ahmad, A., Ripin, A., 2017b. Composite membranes based on heteropolyacids and their applications in fuel cells. In: Organic-Inorganic Composite Polymer Electrolyte Membranes. Springer International Publishing, Cham, pp. 99–131. 10.1007/978-3-319-52739-0_5.

Assumma, L., Iojoiu, C., Mercier, R., Lyonnard, S., Nguyen, H.D., Planes, E., 2015. Synthesis of partially fluorinated poly(arylene ether sulfone) multiblock copolymers bearing perfluorosulfonic functions. J. Polym. Sci. Part A Polym. Chem. 53, 1941–1956. https://doi.org/10.1002/pola.27650.

Che, Q., Zhu, Z., Chen, N., Zhai, X., 2015a. Methylimidazolium group – Modified polyvinyl chloride (PVC) doped with phosphoric acid for high temperature proton exchange membranes. Mater. Des. 87, 1047–1055. https://doi.org/10.1016/j.matdes.2015.08.092.

Che, Q.T., Zhou, L., Wang, J.L., 2015b. Fabrication and characterization of phosphoric acid doped imidazolium ionic liquid polymer composite membranes. J. Mol. Liq. 206, 10–18. https://doi.org/10.1016/j.molliq.2015.01.054.

Chen, H., Han, S.-Y., Liu, R.-H., Chen, T.-F., Bi, K.-L., Liang, J.-B., Deng, Y.-H., Wan, C.-Q., 2018. High conductive, long-term durable, anhydrous proton conductive solid-state electrolyte based on a metal-organic framework impregnated with binary ionic liquids: synthesis, characteristic and effect of anion. J. Power Sources 376, 168–176. https://doi.org/10.1016/j.jpowsour.2017.11.089.

Diaz, M., Ortiz, A., Ortiz, I., 2014. Progress in the use of ionic liquids as electrolyte membranes in fuel cells. J. Membr. Sci. 469, 379–396. https://doi.org/10.1016/j.memsci.2014.06.033.

Díaz, M., Ortiz, A., Vilas, M., Tojo, E., Ortiz, I., 2014. Performance of PEMFC with new polyvinyl-ionic liquids based membranes as electrolytes. Int. J. Hydrogen Energy 39, 3970–3977. https://doi.org/10.1016/j.ijhydene.2013.04.155.

Fang, J., Lyu, M., Wang, X., Wu, Y., Zhao, J., 2015. Synthesis and performance of novel anion exchange membranes based on imidazolium ionic liquids for alkaline fuel cell applications. J. Power Sources 284, 517–523. https://doi.org/10.1016/j.jpowsour.2015.03.065.

Fernicola, A., Scrosati, B., Ohno, H., 2006. Potentialities of ionic liquids as new electrolyte media in advanced electrochemical devices. Ionics (Kiel) 12, 95–102. https://doi.org/10.1007/s11581-006-0023-5.

Gajos, K., Guzenko, V.A., Dübner, M., Haberko, J., Budkowski, A., Padeste, C., 2016. Electron-beam lithographic grafting of functional polymer structures from fluoropolymer substrates. Langmuir 32, 10641–10650. https://doi.org/10.1021/acs.langmuir.6b02808.

Gold, S.A., 2017. Low-temperature fuel cell technology for green energy. In: Handbook of Climate Change Mitigation and Adaptation. Springer International Publishing, Cham, pp. 3039–3085. 10.1007/978-3-319-14409-2_43.

Gong, F., Wang, R., Chen, X., Chen, P., An, Z., Zhang, S., 2017. Facile synthesis and the properties of novel cardo poly(arylene ether sulfone)s with pendent cycloaminium side chains as anion exchange membranes. Polym. Chem. 8, 4207–4219. https://doi.org/10.1039/C7PY00690J.

Gubler, L., 2014. Polymer design strategies for radiation-grafted fuel cell membranes n/a–n/a Adv. Energy Mater. 4. https://doi.org/10.1002/aenm.201300827.

Guerreiro da Trindade, L., Regina Becker, M., Celso, F., Petzhold, C. L., Martini, E.M.A., de Souza, R.F., 2016. Modification of sulfonated poly(ether ether ketone) membranes by impregnation with the ionic liquid 1-butyl-3-methylimidazolium tetrafluoroborate for proton exchange membrane fuel cell applications. Polym. Eng. Sci. 56, 1037–1044. https://doi.org/10.1002/pen.24334.

Güler, E., Sadeghi, S., Alkan Gürsel, S., 2018. Characterization and fuel cell performance of divinylbenzene crosslinked phosphoric acid doped membranes based on 4-vinylpyridine grafting onto poly (ethylene-co-tetrafluoroethylene) films. Int. J. Hydrogen Energy 43, 8088–8099. https://doi.org/10.1016/j.ijhydene.2018.03.087.

Hu, Y., Li, X., Yan, L., Yue, B., 2017. Improving the overall characteristics of proton exchange membranes via nanophase separation technologies: a progress review. Fuel Cells 17, 3–17. https://doi.org/10.1002/fuce.201600172.

Ishioka, Y., Minakuchi, N., Mizuhata, M., Maruyama, T., 2014. Supramolecular gelators based on benzenetricarboxamides for ionic liquids. Soft Matter 10, 965–971. https://doi.org/10.1039/C3SM52363B.

Jothi, P.R., Dharmalingam, S., 2014. An efficient proton conducting electrolyte membrane for high temperature fuel cell in aqueous-free medium. J. Membr. Sci. 450, 389–396. https://doi.org/10.1016/j.memsci.2013.09.034.

Kataoka, T., Ishioka, Y., Mizuhata, M., Minami, H., Maruyama, T., 2015. Highly conductive ionic-liquid gels prepared with orthogonal double networks of a low-molecular-weight gelator and cross-linked polymer. ACS Appl. Mater. Interfaces 7, 23346–23352. https://doi.org/10.1021/acsami.5b07981.

Kim, D.J., Jo, M.J., Nam, S.Y., 2015. A review of polymer - nanocomposite electrolyte membranes for fuel cell application. J. Ind. Eng. Chem. 21, 36–52. https://doi.org/10.1016/j.jiec.2014.04.030.

Kim, D.W., Chi, D.Y., 2004. Polymer-supported ionic liquids: imidazolium salts as catalysts for nucleophilic substitution reactions including fluorinations. Angew. Chemie – Int. Ed. 43, 483–485. https://doi.org/10.1002/anie.200352760.

Kim, Y., Choi, Y., Kim, H.K., Lee, J.S., 2010. New sulfonic acid moiety grafted on montmorillonite as filler of organic-inorganic composite membrane for non-humidified proton-exchange membrane fuel cells. J. Power Sources 195, 4653–4659. https://doi.org/10.1016/j.jpowsour.2010.01.087.

Kreuer, K.D., 2001. On the development of proton conducting polymer membranes for hydrogen and methanol fuel cells. J. Membr. Sci. 185, 29–39. https://doi.org/10.1016/S0376-7388(00)00632-3.

Kurane, R., Jadhav, J., Khanapure, S., Salunkhe, R., Rashinkar, G., 2013. Synergistic catalysis by an aerogel supported ionic liquid phase (ASILP) in the synthesis of 1,5-benzodiazepines. Green Chem. 15, 1849. https://doi.org/10.1039/c3gc40592c.

MacFarlane, D.R., Tachikawa, N., Forsyth, M., Pringle, J.M., Howlett, P.C., Elliott, G.D., Davis, J.H., Watanabe, M., Simon, P., Angell, C.A., 2014. Energy applications of ionic liquids. Energy Environ. Sci. 7, 232–250. https://doi.org/10.1039/C3EE42099J.

Madden, T., Perry, M., Protsailo, L., Gummalla, M., Burlatsky, S., Cipollini, N., Motupally, S., Jarvi, T., 2010. Proton exchange membrane fuel cell degradation: mechanisms and recent progress. In: Handbook of Fuel Cells. John Wiley & Sons, Ltd, Chichester, UK. 10.1002/9780470974001.f500057.

Mecerreyes, D., 2011. Polymeric ionic liquids: broadening the properties and applications of polyelectrolytes. Prog. Polym. Sci. 36, 1629–1648. https://doi.org/10.1016/j.progpolymsci.2011.05.007.

Miyake, J., Miyatake, K., 2017. Fluorine-free sulfonated aromatic polymers as proton exchange membranes. Polym. J. 49, 487–495. https://doi.org/10.1038/pj.2017.11.

Nasef, M.M., 2014. Radiation-grafted membranes for polymer electrolyte fuel cells: current trends and future directions. Chem. Rev. 114, 12278–12329. https://doi.org/10.1021/cr4005499.

Nasef, M.M., Fujigaya, T., Abouzari-Lotf, E., Nakashima, N., 2017. Electrospinning of poly(vinylpyrrodine) template for formation of ZrO_2 nanoclusters for enhancing properties of composite proton conducting membranes. Int. J. Polym. Mater. Polym. Biomater. 66, 289–298. https://doi.org/10.1080/00914037.2016.1201829.

Nasef, M.M., Fujigaya, T., Abouzari-Lotf, E., Nakashima, N., Yang, Z., 2016. Enhancement of performance of pyridine modified polybenzimidazole fuel cell membranes using zirconium oxide nanoclusters and optimized phosphoric acid doping level. Int. J. Hydrogen Energy 41, 6842–6854. https://doi.org/10.1016/j.ijhydene.2016.03.022.

Osada, I., de Vries, H., Scrosati, B., Passerini, S., 2016. Ionic-liquid-based polymer electrolytes for battery applications. Angew. Chemie Int. Ed. 55, 500–513. https://doi.org/10.1002/anie.201504971.

Park, M.J., Lee, J.K., Lee, B.S., Lee, Y.-W., Choi, I.S., Lee, S., 2006. Covalent modification of multiwalled carbon nanotubes with imidazolium-based ionic liquids: effect of anions on solubility. Chem. Mater. 18, 1546–1551. https://doi.org/10.1021/cm0511421.

Ponce-González, J., Whelligan, D.K., Wang, L., Bance-Soualhi, R., Wang, Y., Peng, Y., Peng, H., Apperley, D.C., Sarode, H.N., Pandey, T.P., Divekar, A.G., Seifert, S., Herring, A.M., Zhuang, L., Varcoe, J.R., 2016. High performance aliphatic-heterocyclic benzyl-quaternary ammonium radiation-grafted anion-exchange membranes. Energy Environ. Sci. 9, 3724–3735. https://doi.org/10.1039/C6EE01958G.

Quartarone, E., Angioni, S., Mustarelli, P., 2017. Polymer and composite membranes for proton-conducting, high-temperature fuel cells: a critical review. Materials (Basel) 10, 687. https://doi.org/10.3390/ma10070687.

Rhoades, T.C., Wistrom, J.C., Daniel Johnson, R., Miller, K.M., 2016. Thermal, mechanical and conductive properties of imidazolium-containing thiol-ene poly(ionic liquid) networks. Polymer (Guildf) 100, 1–9. https://doi.org/10.1016/j.polymer.2016.08.010.

Schultz, M.G., 2003. Air pollution and climate-forcing impacts of a global hydrogen economy. Science (80-.) 302, 624–627. https://doi.org/10.1126/science.1089527.

Sekhon, S.S., Lalia, B.S., Park, J.-S., Kim, C.-S., Yamada, K., 2006. Physicochemical properties of proton conducting membranes based on ionic liquid impregnated polymer for fuel cells. J. Mater. Chem. 16, 2256. https://doi.org/10.1039/b602280d.

Sproll, V., Schmidt, T.J., Gubler, L., 2018. Effect of glycidyl methacrylate (GMA) incorporation on water uptake and conductivity of proton exchange membranes. Radiat. Phys. Chem. 144, 276–279. https://doi.org/10.1016/j.radphyschem.2017.08.025.

Su, D.S., Perathoner, S., Centi, G., 2013. Nanocarbons for the development of advanced catalysts. Chem. Rev. 113, 5782–5816. https://doi.org/10.1021/cr300367d.

Tan, N., Chen, Y., Xiao, G., Yan, D., 2010. Synthesis and properties of sulfonated polybenzothiazoles with benzimidazole moieties as proton exchange membranes. J. Membr. Sci. 356, 70–77. https://doi.org/10.1016/j.memsci.2010.03.028.

Uragami, T., Fukuyama, E., Miyata, T., 2016. Selective removal of dilute benzene from water by poly(methyl methacrylate)-graft-poly(dimethylsiloxane) membranes containing hydrophobic ionic liquid by pervaporation. J. Membr. Sci. 510, 131–140. https://doi.org/10.1016/j.memsci.2016.01.057.

Valkenberg, M.H., deCastro, C., Hölderich, W.F., 2002. Immobilisation of ionic liquids on solid supports. Green Chem. 4, 88–93. https://doi.org/10.1039/b107946h.

Wang, J., Luo, J., Feng, S., Li, H., Wan, Y., Zhang, X., 2016. Recent development of ionic liquid membranes. Green Energy Environ. 1, 43–61. https://doi.org/10.1016/j.gee.2016.05.002.

Wojnarowska, Z., Knapik, J., Díaz, M., Ortiz, A., Ortiz, I., Paluch, M., 2014. Conductivity mechanism in polymerized imidazolium-based protic ionic liquid [HSO_3–BVIm][OTf]: dielectric relaxation studies. Macromolecules 47, 4056–4065. https://doi.org/10.1021/ma5003479.

Wu, W., Li, Y., Chen, P., Liu, J., Wang, J., Zhang, H., 2016. Constructing ionic liquid-filled proton transfer channels within nanocomposite membrane by using functionalized graphene oxide. ACS Appl. Mater. Interfaces 8, 588–599. https://doi.org/10.1021/acsami.5b09642.

Xin, B., Hao, J., 2014. Imidazolium-based ionic liquids grafted on solid surfaces. Chem. Soc. Rev. 43, 7171–7187. https://doi.org/10.1039/C4CS00172A.

Yamamoto, Y., Higashi, S., Yamamoto, K., 2008. XPS-depth analysis using C 60 ion sputtering of buried interface in plasma-treated ethylene-tetrafluoroethylene-copolymer (ETFE) film. Surf. Interface Anal. 40, 1631–1634. https://doi.org/10.1002/sia.2884.

Yasuda, T., Nakamura, S., Honda, Y., Kinugawa, K., Lee, S.-Y., Watanabe, M., 2012. Effects of polymer structure on properties of sulfonated polyimide/protic ionic liquid composite membranes for nonhumidified fuel cell applications. ACS Appl. Mater. Interfaces 4, 1783–1790. https://doi.org/10.1021/am300031k.

Ye, Y.-S., Rick, J., Hwang, B.-J., 2013. Ionic liquid polymer electrolytes. J. Mater. Chem. A 1, 2719–2743. https://doi.org/10.1039/C2TA00126H.

Zakeri, M., Abouzari-Lotf, E., Nasef, M.M., Ahmad, A., Ripin, A., Ting, T.M., Sithambaranathan, P., 2018. Preparation and characterization of highly stable protic-ionic-liquid membranes. Int. J. Hydrogen Energy. https://doi.org/10.1016/j.ijhydene.2018.04.015.

Zhang, L., Chae, S.-R., Hendren, Z., Park, J.-S., Wiesner, M.R., 2012. Recent advances in proton exchange membranes for fuel cell applications. Chem. Eng. J. 204–206, 87–97. https://doi.org/10.1016/j.cej.2012.07.103.

Zhang, Y., Li, J., Ma, L., Cai, W., Cheng, H., 2015. Recent developments on alternative proton exchange membranes: strategies for systematic performance improvement. Energy Technol. 3, 675–691. https://doi.org/10.1002/ente.201500028.

Zheng, W., Wang, L., Deng, F., Giles, S.A., Prasad, A.K., Advani, S.G., Yan, Y., Vlachos, D.G., 2017. Durable and self-hydrating tungsten carbide-based composite polymer electrolyte membrane fuel cells. Nat. Commun. 8, 418. https://doi.org/10.1038/s41467-017-00507-6.

Zhu, X., Liu, Y., Zhu, L., 2008. Polymer composites for high-temperature proton-exchange membrane fuel cells. In: Polymer Membranes for Fuel Cells. Springer US, Boston, MA, pp. 1–26. 10.1007/978-0-387-73532-0_7.

Zhuo, Y.Z., Lai, A.L., Zhang, Q.G., Zhu, A.M., Ye, M.L., Liu, Q.L., 2015. Enhancement of hydroxide conductivity by grafting flexible pendant imidazolium groups into poly(arylene ether sulfone) as anion exchange membranes. J. Mater. Chem. A 3, 18105–18114. https://doi.org/10.1039/C5TA04257G.